Publicado en RSC Advances 5,55784-55794 (2015)

Comparison of hydrocarbon- and lactam-bridged cyclic peptides as dimerization inhibitors of *Leishmania infantum* trypanothione reductase†

Pedro A. Sánchez-Murcia,[a] Marta Ruiz-Santaquiteria,[b] Miguel A. Toro,[c] Héctor de Lucio,[c] María Ángeles Jiménez,[d] Federico Gago,[a] Antonio Jiménez-Ruiz,[c] María-José Camarasa,[b] and Sonsoles Velázquez[b]*

A table of contents entry

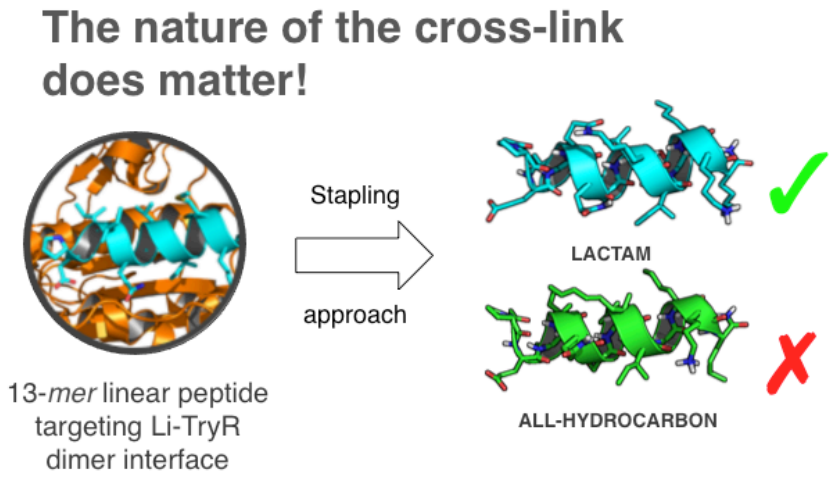

Helical peptides stabilized via all-hydrocarbon or lactam side-chain bridging were investigated as disruptors of *Leishmania infantum* trypanothione reductase and the biological results were rationalized by NMR spectroscopy studies and molecular dynamic simulations.

Abstract— All-hydrocarbon and lactam-bridged staples linking amino acid side-chains have been used to stabilize the α-helical motif in short 13-mer peptides that target critical protein-protein interactions at the dimerization interface of *Leishmania infantum* trypanothione reductase (Li-TryR). The design of the best positions for covalent hydrocarbon closure relied on a theoretical prediction of the degree of helicity of the corresponding cyclic peptides in water. Selected *(i, i+4)* and *(i, i+7)* hydrocarbon-stapled peptides were prepared by using solid-phase synthesis protocols and optimized ring-closing metathesis reactions under microwave conditions. Structural analysis by NMR spectroscopy confirmed high helical contents in aqueous TFE solutions for both types of helix-constrained cyclic peptides. Remarkably, the ability to reduce Li-TryR dimerization was reduced in both *(i, i+4)* and *(i, i+7)* hydrocarbon stapled peptides but was retained in the corresponding *(i, i+4)* Glu-Lys lactam-bridged analogue which also showed a higher resistance to proteolytic degradation by proteinase K relative to the linear peptide prototype. *In silico* studies indicated that the introduction of a hydrocarbon staple *vs* a lactam bridge likely perturbs critical interactions required for proper binding of the peptide to the Li-TryR monomer.

Keywords- peptides, helix stabilization, peptide structure, protein-protein interactions, trypanothione reductase, leishmania

Introduction

Leishmaniasis is a parasitic infection caused by unicellular protozoan organisms (*Leishmania spp.)* belonging to the Trypanosomatidae family. Although this disease is seen nowadays as a global health problem,[1] currently available drugs are decades old and have several drawbacks including poor efficiency and bioavailability, toxicity to humans, high cost, and the emergence of drug-resistant parasitic strains.[2-5] Thus, there is an urgent need to

find new targets and/or inhibition mechanisms against these parasites. Trypanothione reductase (TryR) is an essential enzyme for survival in trypanosomatids that is used to maintain the dithiol of trypanothione [bis(glutathionil spermidine)] in its reduced state.[6-8] Because of the lack of catalase and glutathione peroxidase activities, these parasites rely solely on the trypanothione system as a defense mechanism against the oxidative stress that is generated either by their own metabolism or by the host immune response.

In addition to playing a pivotal role in the parasite, another characteristic that makes TryR a potential target for antiparasitic drugs is the different substrate specificity from that of glutathione reductase, the enzyme with the most similar function in humans. These facts make TryR a very attractive validated target for drug development against trypanosomatid-caused infections. Several inhibitors of TryR have been reported including those based on tricyclic antidepressants,[9-10] polyamine conjugates[11,12] and substrate analogues.[9-14] Most of the efforts to inhibit TryR have relied on the design of molecules directed towards the active site but with limited success. Taking advantage of the fact that the functional form of TryR is a homodimer, we have recently reported an alternative inhibition strategy aimed at disrupting the dimer interface of the enzyme by means of protein-protein interaction inhibitors[15] (Figure 1). By a combination of molecular modelling and site-directed mutagenesis studies we identified and validated E436 as a key amino acid (hot spot) for the structural stability and function of the dimer. On the basis of these results and as a "proof of concept" of this novel approach we designed and tested a small library of linear peptides whose sequences were directly derived from the helical homodimerization domain containing E436 (residues P435-M447) of *Leishmania infantum* TryR (Li-TryR). Among the synthesized peptides, the linear PEIIQSVGISMKM (**1**) and PEIIQSVGIS-Nle-K-Nle (**2**) 13-*mers*, in which a Cys and/or the two Met residues of the wild-type peptide sequence were replaced by isosteric Ser

and Nle (in order to prevent potential oxidation), stood out as promising Li-TryR dimerization inhibitors in the micromolar range (Fig. 1).[15]

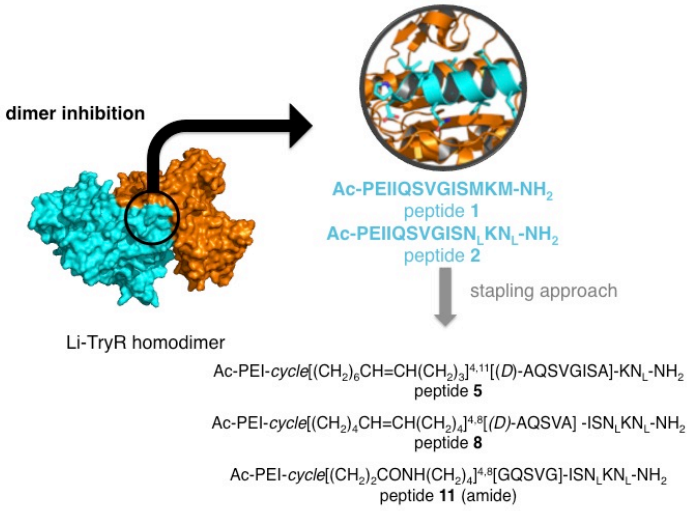

Fig. 1. Li-TryR dimer inhibition strategy and designed stapled peptides synthesized in this work. N_L: *norleucine*.

Covalent side-chain to side-chain linkage ("stapling") within small α-helical segments derived from a protein has allowed to overcome the little or no helical character shown in solution by these oligopeptides when they are excised from their native context.[16] Thus, incorporation of both lactam bridges[17-19] and short hydrocarbon chains[20-21] as staples has been shown to enhance helicity, resistance to proteolysis and cell permeability. To date, numerous examples of stapled peptides with affinity for several therapeutic targets and the ability to modulate protein-protein interactions have been reported.[22,23]

In order to stabilize the α-helical structure of the short linear prototype **2**, we herein describe our initial studies of the effects of side-chain hydrocarbon stapling (peptides **5** and **8**) [at either one *(i, i+4)* or two turns *(i, i+7)* of the α-helix] or incorporation of a lactam bridge (peptide **11**) (Fig. 1) on (i) the peptide helical conformation, (ii) the proteolytic stability, and (iii) the ability to disrupt Li-TryR dimerization. Our data show that the all-

hydrocarbon stapled peptides are inactive in Li-TryR dimerization assays whereas the lactam-bridged cyclic peptide stands out as a potent inhibitor of TryR dimerization. A rationale for these significant differences was provided by analysing the results obtained from molecular dynamics (MD) simulations in explicit solvent.

Results and Discussion

In silico design of stapled peptides

From available helix stabilization strategies,[16,17] we first selected the all-hydrocarbon stapling approach developed by Verdine and colleagues.[21] It is well established that for *i,i+4* or *i,i+7* stapling, the most stereochemically favourable cross-link to stabilise helices is through two units of (*S*)-α-methyl-α-pentenylglycine (**3**) to form $S_{i,i+4}S(8)$[24] staples or between one unit of (*R*)-α-methyl-α-octenylglycine (**4**) (Figure in Table 1) and one unit of 3 to form $R_{i,i+7}S(11)$[25] staples according to the nomenclature described by Verdine et al. [21a] Since the staple position critically influences the overall degree of structure and biological activity of a given peptide,[21a,26] we first performed an *in silico* analysis to select the best positions for covalent *i,i+4* and *i,i+7* closures that would lead to a higher degree of stabilization of the helical structure in linear peptide **2** (Table 1). All the staples in peptide **2** were placed on the face opposite to that used for binding to the Li-TryR monomer so as to preserve the crucial interactions at the interface.

Table 1 highlights all possible positions in the sequence of **2** for the introduction of the non-natural α,α-disubstituted residues bearing the double bonds (**3** and **4**) which would lead to the hydrocarbon bridge after ruthenium-catalyzed ring closing metathesis (stapled peptides **5**-**10**). There are six possible stapled peptides: **5** and **6** (*i, i+7* staples) and **7**-**10** (*i, i+4* staples).

Table 1. Chemical structure of non-proteinogenic amino acids (*S*)-**3** and (*R*)-**4** and helical wheel projection of linear peptide prototype **2** onto the Li-TryR monomer showing all possible stapling positions at the non-recognition side that would lead to stapled peptides **5-10**.

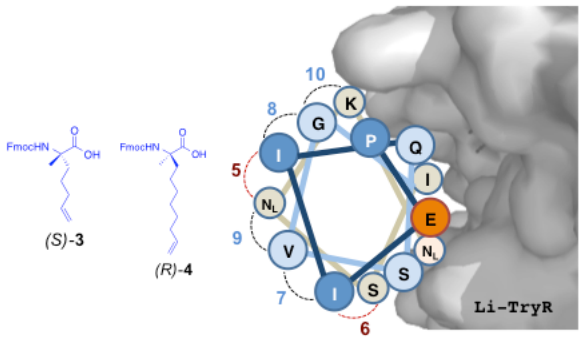

Peptides	*Position*												
	1	*2*	*3*	*4*	*5*	*6*	*7*	*8*	*9*	*10*	*11*	*12*	*13*
1 (linear)	P	E	I	I	Q	S	V	G	I	S	M	K	M
2 (prototype)	P	E	I	I	Q	S	V	G	I	S	N_L	K	N_L
5	P	E	I	**4**	Q	S	V	G	I	S	**3**	K	N_L
6	P	E	**4**	I	Q	S	V	G	I	**3**	N_L	K	N_L
7	P	E	**3**	I	Q	S	**3**	G	I	S	N_L	K	N_L
8	P	E	I	**3**	Q	S	V	**3**	I	S	N_L	K	**N_L**
9	P	E	I	I	Q	S	**3**	G	I	S	**3**	K	N_L
10	P	E	I	I	Q	S	V	**3**	I	S	N_L	**3**	N_L

N_L: *norleucine*.

Stapled peptides **5**-**10** showed increased degrees of predicted helicity per residue compared to the linear peptide **2** (Fig. 2). In addition, significant differences were found depending on the position and the length of the hydrocarbon staples.

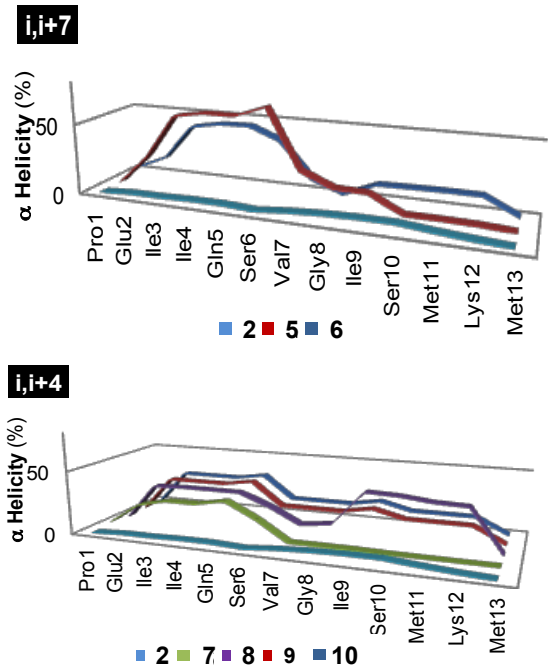

Fig. 2. Predicted α-helicities per residue (%) of peptides **5-10** and **2** (prototype) calculated with the *dssp* algorithm.

In general, the *i, i+7* stapling system was found to be more stabilizing than *i, i+4* in terms of absolute helicity values. Among the possible *i, i+7* staples, peptide **5** displayed the highest α-helix propensity towards the *N*-terminus, reaching absolute values close to 50% helicity (Fig. 2, in red). On the other hand, peptide **8** with the *i, i+4* staple located at the centre of the helix (Fig. 2, in purple) exhibited the highest α-helix stabilization towards the C-terminus. On the basis of these findings, stapled peptides **5** and **8** (linking positions 4 and 11 and 4 and 8, respectively) were selected for synthesis and further study.

For comparative purposes, the constrained *i, i+4* cyclic analogue with a lactam bridge between the side-chains of Glu-Lys residues at positions 4 and 8 [Ac-PEI(EQSVK)IS-Nle-K-Nle-NH_2 (**11**)] was also selected for study. This enabled us to compare the effects of hydrocarbon versus lactam linkers on helix stabilization and on Li-TryR dimerization disruption.

Chemical synthesis

For hydrocarbon-stapled peptides, we first synthesized the required optically pure α,α-disubstituted amino acids (*S*)-**3** and (*R*)-**4**. This was made from the commercially available chiral diphenyloxazinones following the procedure described by Williams and colleagues[27] and the modifications reported by Verdine group.[21a] In brief, two consecutive asymmetric alkylations on C-3, scaffold cleavage, and final Fmoc protection of the *N*-terminal amino acid gave the desired quaternary amino acids (*S*)-**3** and (*R*)-**4** (Scheme S1, Supporting Information).

Target stapled peptides **5** and **8** were synthesized manually following the standard Fmoc/tBu solid-phase orthogonal protection strategy on Rink amide-MBHA polystyrene resin (Scheme 1). The appropriate α-methyl-α-alkenylamino acids were introduced at the right positions of the sequence in the elongation step. Dicarba bridge formation was accomplished from the linear precusors **12** and **13** through on-resin ring-closing metathesis (RCM) using Grubb's second-generation ruthenium catalyst. The optimal microwave conditions for the RCM reaction were 100 °C using 20 mol% of catalyst, LiCl as a chaotropic agent[28] and CH_2Cl_2 as the solvent. Next, the *N*-terminus of the peptides was acetylated and cleaved from the resin under standard conditions.

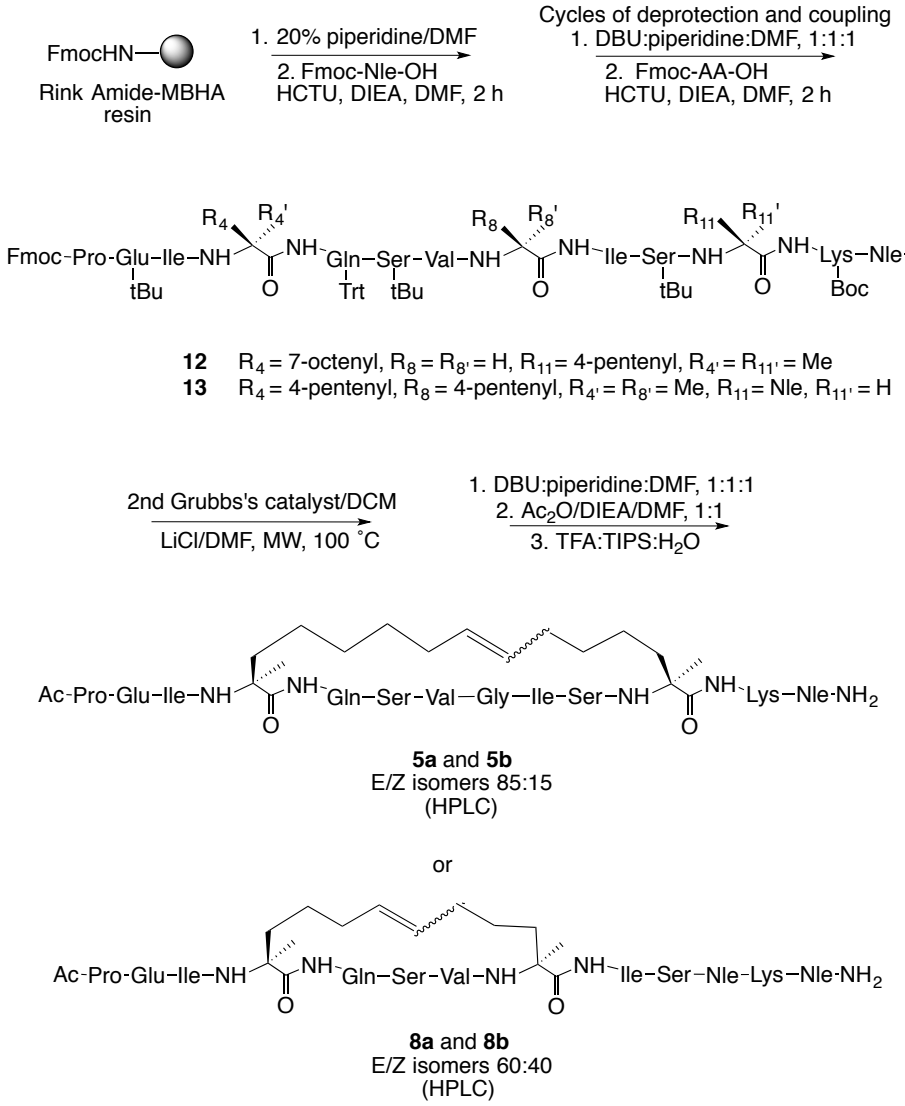

Scheme 1. Synthesis of target stapled peptides **5a,b** and **8a,b.**

The crude peptides were purified on reverse phase solid-phase extraction (SPE) cartridges or semipreparative high performance liquid chromatography (HPLC) to give the desired stapled peptides **5** and **8** in 30% and 6% overall yields, respectively. Both *E* and *Z* isomers were detected by HPLC in 85:15 and 60:40 ratios for **5** and **8**, respectively, and could be partially separated. The major isomers **5a** and **8a** very probably corresponds to the *E* isomers since the NMR coupling constant $^{3}J_{HH}$ between the vinyl protons is approximately 13-15 Hz.

Inhibition of Li-TryR dimerization

The effects on dimer stability of the (*i, i+4* or *i, i+7*)-hydrocarbon stapled peptides **5a** (major isomer), **8a** (major isomer), **8a,b** (mixture of isomers) and the (*i, i+4*) lactam-bridged analogue **11**, and the linear prototype peptide **2** were evaluated by using a highly sensitive and versatile in-house ELISA[15] (Table 2). These studies revealed that all-hydrocarbon stapled analogues **5a, 8a** and **8a,b** did not significantly induce disruption of the Li-TryR dimer. In contrast, the lactam-bridged analogue **11** reduced the detection of labeled Li-TryR dimer to the same extent that did their linear counterpart **2**. Thus, even when the same positions are stapled (**8a** or **8a,b** *vs* **11**), the nature of the covalent linkage has a deep impact on the potency of the peptides as Li-TryR dimerization disruptors.

Table 2. Potency of linear peptide **2** and cyclic peptides **5a, 8a, 8a,b** and **11** in the Li-TryR monomer displacement assay.

Peptide	IC_{50} (μM)[a]
2 (linear prototype)	15.6 ± 1.4
5a (major isomer; 4,11-hydrocarbon-stapled)	> 75
8a (major isomer; 4,8-hydrocarbon-stapled)	> 75
8a,b (mixture of isomers; 4,8-hydrocarbon-stapled)	> 75
11 (4,8-lactam-bridged)	24.8 ± 0.4
Mepacrine (control)	> 75

[a] Results are representative of three independent experiments each performed in triplicate. >75 indicates that IC_{50} is higher than 75 μM (maximum assayed)

NMR structural studies

In order to elucidate whether the nature of the covalent linkage could have a differential effect on the structure of the all-hydrocarbon-stapled **8** and lactam-bridged **11** peptides we examined the structural behaviour of these peptides in solution by 1D and 2D NMR spectroscopy. In particular, we selected the lactam-bridged derivative **11** and the major geometric isomer of peptide **8a** (isomer *E* according to a NMR coupling constant $^{3}J_{HH}$ between the vinyl protons > 15 Hz). Both peptides **8a** and **11**, in the TFE/H_2O solvent,[29] showed medium-range NOE cross-peaks characteristic of α-helices, i.e. $d\alpha N_{(i,i+2)}$, $d\alpha N_{(i,i+3)}$, $d\alpha N_{(i,i+4)}$, and $d\alpha\beta_{(i,i+3)}$ (Fig. 3). As an example, a detail of the $^{1}H,^{1}H$-NOESY spectra of **8a** and **11** is shown in Fig. 3A, B. Additionally, the deviations of chemical shifts from random coil values shown by the Hα protons ($\Delta\delta_{H\alpha} = \delta_{H\alpha}$ observed – $\delta_{H\alpha}$ random coil, ppm) are positive and large in magnitude (Fig. S1), which are also characteristic of helices. The percentages of helix formed by peptides **8a** and **11** in 30% TFE at pH 5.5 and 25 ºC are 71% and 88%, respectively, as estimated from the averaged $\Delta\delta_{H\alpha}$ values.[30]

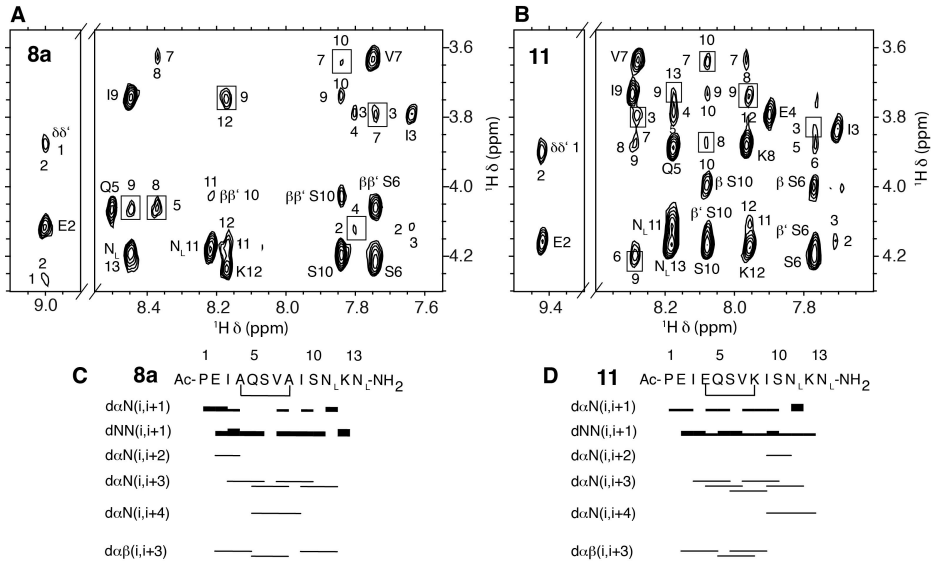

Fig. 3. Detail of the 2D $^{1}H,^{1}H$-NOESY spectrum of **8a** (A) and **11** (B) in 30% TFE in H_2O/D_2O 9:1 v/v at pH 5.5 and 25ºC. The intra-residue αN(i,i+1) and sequential αN(i,i+1) NOE cross-peaks are labelled and the medium-range αN(i,i+2) and αN(i,i+3) NOE cross-peaks are also boxed. (C) NOE summary of **8a**. (D) NOE summary of **11**.

Given the large helical populations presented by stapled peptides **8a** and **11**, and to visualize their 3D structure, we next performed structure calculations from geometric constraints (distances and dihedral angles; Table S1) derived from NMR parameters and using the CYANA program.[31] The ensemble of the 20 lowest target function conformers resulting for each peptide was well defined, as seen in Fig. 4, and indicated by the pairwise root mean square deviation (RMSD), which is 0.50 ± 0.20 and 0.60 ± 0.20 Å for the backbone atoms of peptides **8a** and **11**, respectively (Table S1).

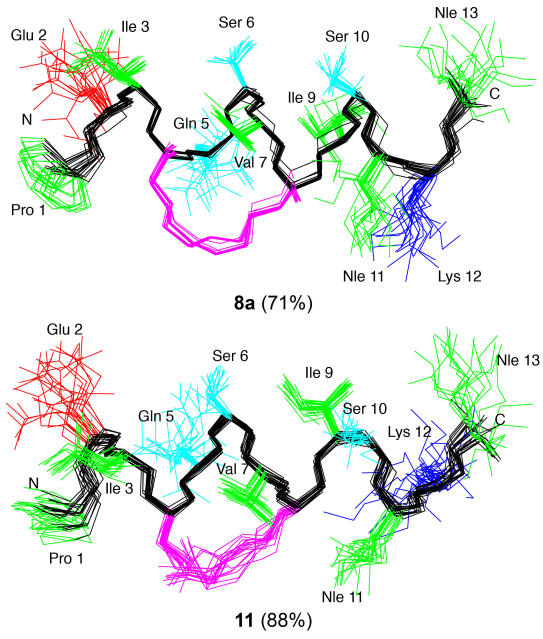

Fig. 4. Superimposition of the 20 lowest target function calculated structures for peptides **8a** and **11** and their helix population (%) in solution (in brackets). Backbone atoms are shown in black. Covalent closures are highlighted in magenta.

On the other hand, the superimposition of the two best calculated structures for cyclic peptides **8a** and **11** with the Li-TryR α-helix Pro435-Met447 in the native protein shows a

correct orientation of the side chains of those residues in the interaction face with the protein (Fig. S2). This confirms our premise that the staple is oriented on the opposite face. However, it is noteworthy that there are no relevant differences in structurating both cyclic peptides as α-helices in TFE/H_2O solution, and therefore, the observed variations in the activity of the peptides as dimer disruptors cannot be attributed to differences in the ability of the staples to stabilize the helical structure in solution.

Molecular modelling

The MD simulation studies (Fig. 5) complemented the NMR solution experiments, as it is known that the conformation of a protein-bound ligand can be different from that found in solution. In this case, we considered both geometric isomers *E*/*Z* of all-hydrocarbon stapled peptides **5a,b** and **8a,b,** the lactam-bridged derivative **11** and the linear prototype **2** (used as a control).

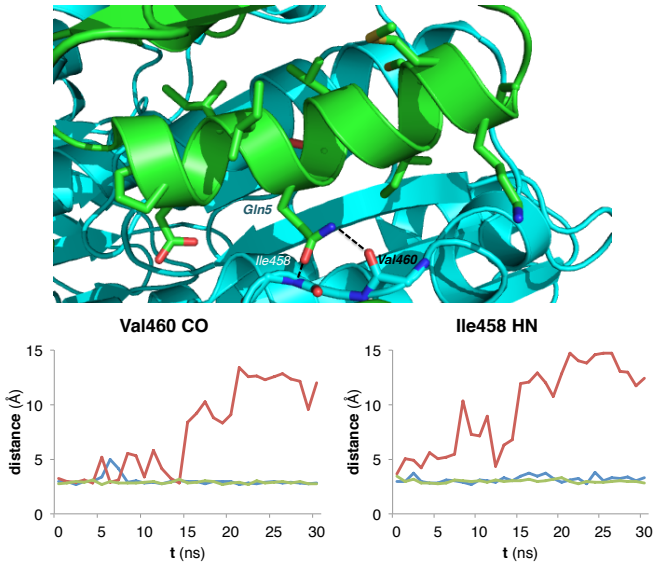

Fig. 5. Evolution of distances (Å) between the Gln5 side chain (carbon atoms coloured in green) of peptide **2** (green), **8a** (red) and **11** (blue) and the Li-TryR monomer (carbon atoms coloured in blue) along their respective MD trajectories.

We have previously shown[15] that the replacement of the Gln side chain at position 5, in similar 13-*mer* peptides, by Ala has the greatest deleterious effect on their potency as Li-TryR inhibitors. Thus, we monitored the interaction of the former residue with the Li-TryR monomer along the different MD trajectories for all the simulated peptides. As an example, Fig. 5 shows the evolution of the distances between the crucial Gln5 side chain of the peptides and the amide O(Val460) and N(Ile458) backbone atoms of Li-TryR monomer for the hydrocarbon-stapled derivative **8a**, the lactam-bridged **11** and the linear counterpart **2**. As can be observed, the introduction of the all-hydrocarbon staple in **8a** (Fig. 5, in red) perturbs the interaction of Gln5 with the Li-TryR monomer when compared with the linear peptide **2**. This is a common feature for the rest of the hydrocarbon-stapled peptides studied along the different MD simulations (data not shown). On the contrary, peptide **11** carrying an amide as the covalent bridge, keeps these interactions to a similar extent as the linear counterpart.

Calculation of the total interaction energies for these peptides, when bound to the Li-TryR monomer along the MD trajectories (Fig. S3 and Table S2), reveals that the introduction of the all-hydrocarbon staple in both double-bond isomers **5** and **8** results in a significant 30% decrease in the total binding energy relative to the linear peptide **2**. Regarding the amide-bridged derivative **11**, reduction in the total binding energy is much smaller (14%). These results are in consonance with the experimental IC_{50} values shown in Table 3. Visual inspection of the representative structures of the major clusters of peptides **2**, **8a,b** and **11** calculated along the MD trajectories (Fig. S4) reveals that the unsaturated all-hydrocarbon stapled **8a,b**, when bound to the protein, do not preserve the helicity at both *N*- and *C*-terminus, in agreement with the fraying observed in the NMR structure of **8a** (Fig. 4). Instead, in **11**, the amide bridge is compatible with a good orientation of Gln5. Thus, the binding differences observed along the MD trajectories can be attributed to the hydrophobic

nature of the hydrocarbon linker. Hydrocarbon stapling technology is generally considered as an effective tool to increase the affinity of α-helical peptides for their targets. However, there are reported examples demonstrating that disruption of stabilizing intramolecular interactions between side-chains[32] or reduction of the flexibility in the stapled peptide[33] can prevent adoption of the conformation needed for efficient binding to their target relative to the unstapled peptide. Thus, our studies complement these previous observations that peptide stapling with a view to increase helicity does not necessarily result in enhanced binding affinity for the target protein.

Proteolytic stability

Cleavage by proteases is one of the main pathways for inactivation of peptides in a biological setting. Because proteases bind to their substrates in an extended rather than in a helical conformation, increasing or maintaining a helical conformation is expected to confer proteolytic stability. To determine the influence of lactam-bridged stabilization on proteolytic stability of the peptides, we compared the susceptibilities of the linear prototype peptide **2** and the active lactam-bridged analogue **11** towards degradation by proteinase K, a promiscuous serine protease. The half-live for the lactam-bridge analogue **11** was significantly increased, with calculated $t_{1/2}$ values of 316 min compared to 23 min for the linear peptide **2**.[34] This 14-fold improvement could be due to the increased α-helical character of the cyclic analogue and/or to the presence of the bridge itself, which would be expected to sterically affect the access to protease-sensitive peptide bonds. This result is consistent with previous findings for helix-constrained peptides[35] and makes peptide **11** a new hit that retains the inhibitory potency shown by the linear prototype but it is endowed with improved pharmacokinetic properties.

Conclusions

We have compared two different strategies for covalently linking amino acid side-chains in a short linear peptide (13-*mer*) that targets a hotspot at the dimerization interface of Li-TryR. A series of rationally designed (*i, i+4*) and (*i, i+7*) hydrocarbon stapled derivatives linking amino acids at positions 4 and 8 (peptide **5**) or 4 and 10 (peptide **8**), respectively, and a lactam-bridged analogue of **8** (peptide **11**) were investigated. Although the all-hydrocarbon stapling approach has been reported as successful in many published examples, in our case the hydrocarbon-stapled analogues were not able to disrupt the dimerization process of the enzyme whereas the lactam-bridged analogue **11** maintained the potency of the native linear peptide **2**. Thus, our biological results reveal that the nature of the covalent linker plays a major role in the peptide's ability to prevent Li-TryR dimerization. Structural NMR studies in solution showed that both hydrocarbon and lactam-bridged peptides **8** and **11** display a high α-helical content in TFE/water mixtures. On the other hand, MD simulations of the linear and cyclic analogues bound on the surface of a Li-TryR monomer indicated that the lactam-bridged peptide **11** could maintain the right orientation of the essential Gln5 side-chain better than the hydrocarbon stapled analogue **8**. Thus, our studies represent an example of how the nature of the covalent linkage (hydrocarbon *vs* lactam) may perturb critical interactions required for proper binding to the protein. These findings may be taken into account when designing helix-constrained peptides. Interestingly, the lactam-stabilized analogue **11** not only affords the spatial arrangement of the critical residues in the correct conformation for activity but also provides higher proteolytic stability (14-fold) in comparison to its linear peptide counterpart.

Experimental

Chemistry

Unless otherwise noted, analytical grade solvents and commercially available reagents were used without further purification. DMF and CH_2Cl_2 were dried using activated molecular sieves. Water sensitive reactions were carried out under Ar atmosphere. Chiral diphenyloxazinones, Grubb's second-generation ruthenium catalyst, HCTU, DIEA, piperidine, sodium hexamethyldisilylamide, lithium hexamethyldisilylamide and Ac_2O were purchased from Aldrich (Germany), and TFA from Fluka (Germany). Peptide Ac-PEI(EQSVK)IS-Nle-K-Nle-NH_2 (**11**) cyclized through an amide bond between E4 and K8 was purchased from Peptide Protein Research (UK). The pure product was analyzed by HPLC and electrospray ionization mass spectrometry (ESI-MS). Fmoc-protected amino acids were purchased from Fluka, Novabiochem (Merck, Germany) and Iris Biotech (Germany). Fmoc-protected Rink Amide MBHA resin (0.47 mmol/g loading) was purchased from GS Biochem (China). All amino acids used were of the L-configuration. Linear precursor peptides **12** and **13** were synthesized manually on a 20-positions manifold (Omega) in a 20-mL polypropylene syringe (Dubelcco) equipped with a porous polyethylene filter following SPPS protocols. The coupling and RCM reactions were carried out on solid phase using microwave radiation in a Biotage Initiator reactor in a 5 mL vial. The rest of the SPPS reactions were stirred using an IKA-100 orbital shaker. After cleavage, the acidic crudes were sedimented in Et_2O on a Hettlich Universal 320R centrifuge at 5000 rpm. All the crude and samples were lyophilized using mixtures H_2O:CH_3CN on a Telstar 8-80 instrument. The monitoring of the reactions was also performed by HPLC/MS through a Waters 12695 HPLC connected to a Waters Micromass ZQ spectrometer. Peptides were purified by reverse-phase flash chromatography using C-18 derivatized silica cartridges (C18 Discovery SPE, Aldrich) in a manifold system or by semipreparative HPLC on a

Waters 600 apparatus using an ACE 5 C18-300 (10 x 250 mm) column at a flow rate of 6 mL/min and a Waters 2487 detector, monitored at 214 nm. Mixtures of CH_3CN (solvent A) and H_2O with 0.05% TFA (solvent B) were used a mobile phase. The purity of the synthesized peptides was checked by an HPLC system (Waters 600 or an Agilent equipment) using in all cases a Sunfire C18 column (4.6 mm x 150 mm, 3.5 μm) and the same solvents as the mobile phase (1.0 mL/min flow). Peak detection was carried out at 214 and 254 nm. High-resolution mass spectra (HRMS) were obtained in an *Agilent 6520 Accurate-Mass Q-TOF LC/MS* mass spectrometer using 1% formic acid MeOH or MeOH/CH_3CN mixtures. ^{1}H- and ^{13}C-NMR spectra were recorded in general in $CDCl_3$, acetone-d_6 or DMSO-d_6 on a *Varian INOVA-400* (400 & 100 MHz), a *Varian MERCURY-400* (400 & 100 MHz), a *Varian UNITY-500* (500 & 125 MHz) or in a *Bruker Avance 600* (600.13 & 150.03 MHz) spectrometer using TMS or DSS as the internal reference. The latter was equipped with a TXI cryoprobe. NMR experiments of helix-constrained analogues **5a**, **8a** and **11** were recorded at 1-2 mM concentration in 30% TFE/H_2O solution. ^{1}H- and ^{13}C-NMR chemical shifts (δ) assignation of the former peptides was performed following the standard sequential assignation method using the SPARKY software.[36] Optical rotation measurements were performed in a *Perkin Elmer* 241 MC using a 1 mL cell at 589 nm (sodium D-line).

Synthetic procedures

Peptide elongation. MBHA-Rink Amide resin (1 equiv) previously swollen in CH_2Cl_2/DMF/CH_2Cl_2/DMF (4 x 0.5 min) was treated with a solution of piperidine:DBU:DMF, 1:1:48 (1 x 1 min) and (3 x 10 min) (incomplete Fmoc deprotection was observed with the standard 20% piperidine in DMF) and the resin was drained and washed with DMF/CH_2Cl_2/DMF/CH_2Cl_2/DMF (4 x 0.5 min). Then, a solution of the

corresponding *N*-Fmoc-protected amino acid (1.2 equiv), HCTU (1.2 equiv) and DIEA (2.4 equiv) in anhydrous DMF (0.5-1.0 mL) was added over the swollen peptidil-resin (1.0 equiv) in anhydrous DMF in a microwave vial (5-10 mL). The coupling reaction was heated at 40 ºC using microwave radiation for 10 min. Each coupling step was repeated 3 times using freshly prepared Fmoc-amino acid/coupling reagent mixtures. After complete couplings, the resin was drained and washed with DMF/CH_2Cl_2 /DMF/CH_2Cl_2 (4 x 0.5 min). Coupling reactions to primary and secondary amines were monitored by the ninhydrin and the chloranil tests, respectively.

Ring closing metathesis (RCM) reaction. To the peptidyl-resins **12** and **13** (0.05-0.07 mmol) swollen in anhydrous CH_2Cl_2 (5 mL) in a microwave vial (5-10 mL) second generation Grubb's catalyst (0.2 equiv) was added and the vial was sealed and gently bubbled with argon. Then, the reaction was heated at 40 ºC using microwave radiation for 30-150 min. The resin was then filtered and washed successively with CH_2Cl_2/MeOH. Residual ruthenium impurities were removed by stirring the resin bound peptide with a solution of DMSO (50 equiv relative to the catalyst) in DMF for 12 h.[37] Finally, the resin was washed with DMF/CH_2Cl_2/MeOH (3 x 0.5 min).

Acetylation and cleavage procedure. The cyclic olefinic peptidil-resins, previously swollen, were treated with 2 mL of 20% piperidine in DMF (1 x 1 min) and (3 x 10 min) and washed with DMF/CH_2Cl_2/DMF/CH_2Cl_2/DMF (4 x 0.5 min). Then, a mixture of acetic anhydride/DIEA/DMF (2 mL, 1:1:1) was added (1 x 1 min) and (4 x 10 min) and washed with DMF/CH_2Cl_2/DMF/CH_2Cl_2/DMF (4 x 0.5 min). The cyclic resin-bounded peptides were then cleaved from the resin by treatment with an acidolitic mixture of TFA:TIPS:H_2O, 90:5:5 (6 mL) for 4 h at room temperature. The filtrates were precipitated from cold diethylether (50 mL), centrifuged at 5000 rpm (3 x 10 min) and lyophilized. The cleaved

products were purified by reverse phase chromatography using SPE cartridges or semipreparative HPLC.

Ac-Pro-Glu-Ile-cycle[$(CH_2)_6CH=CH(CH_2)_3$]^{4,11}[(D)-Ala-Gln-Ser-Val-Gly-Ile-Ser-Ala]-Lys-Nle-NH_2 (5a,b). After elongation of the peptide starting from 0.05 mmol of Rink amide resin, the metathesis reaction was carried out for 30 min following the general protocol under microwave conditions. Then, the cyclic peptide was N-acetylated and cleaved from the resin. The crude was purified by reverse phase chromatography using SPE cartridges to give the cyclic peptide **5a,b** (23.7 mg, 30% overall yield) as a partially solved mixture of E/Z isomers (85/15) in three fractions: major isomer (12.0 mg), minor isomer (1.0 mg) and mixture (10.7 mg). **HPLC** (Waters, 5% to 100% of water in 30 min): 4.06 min (**5a**, major isomer, 92% analytical purity) and 3.89 min (**5b**, minor isomer). Major isomer **5a**: **HRMS** (ESI, +) *m/z*: Calculated for $C_{71}H_{122}N_{16}O_{19}$ 1502.9017; found 752.4580 $[(M+2H)+2]^+$. **^{1}H-NMR** (600 MHz, 30% TFA D_2O:H_2O, 1:9) and **^{13}C-NMR** (150 MHz, 30% TFA D_2O:H_2O, 1:9) in Table S3 (Supporting information).

Ac-Pro-Glu-Ile-cycle[$(CH_2)_4CH=CH(CH_2)_4$]^{4,8}[(D)-Ala-Gln-Ser-Val-Ala]-Ile-Ser-Nle-Lys-Nle-NH_2 (8a,b). After elongation of the peptide starting from 0.07 mmol of Rink amide resin, the metathesis reaction was carried out for 150 min following the general protocol under microwave conditions. After *N*-acetylation and cleavage from the resin, the crude was purified by semipreparative HPLC (Waters, 3% to 30% of water, linear gradient in 27 min) to yield the cyclic derivative **8a,b** (7.8 mg, 6% overall yield) as a partially solved mixture of *E*/*Z* isomers (60:40) in two fractions: major isomer (2.1 mg) and mixture (5.7 mg). **HPLC** (Agilent, 10% to 100% of water in 10 min): 6.68 min (**8a**, major isomer, 90% analytical purity) and 6.49 min (**8b**, minor isomer). Major isomer **8a**: **HRMS** (ESI, +) *m/z*: Calculated for $C_{72}H_{124}N_{16}O_{19}$ 1516.9208; found 759.4669 $([M+2H]/2)^+$. **^{1}H-NMR** (600 MHz, 30% TFA

D_2O:H_2O, 1:9) and **^{13}C-NMR** (150 MHz, 30% TFA D_2O:H_2O, 1:9) in Table S4 (Supporting information).

Ac-Pro-Glu-Ile-cycle[$(CH_2)_4CONH(CH_2)_4$]^{4,8}[Glu-Gln-Ser-Val-Lys]-Ile-Ser-Nle-Lys-Nle-NH_2 (11). This peptide, cyclized through an amide bond between E4 and K8, was purchased from Peptide Protein Research (UK). The pure product was analyzed by HPLC and electrospray ionization mass spectrometry (ESI-MS). **HPLC** (Agilent, 10% to 100% of water in 10 min): 5.98 min, 95% analytical purity. **HRMS** (ESI, +) *m/z*: Calculated for $C_{69}H_{119}N_{17}O_{20}$ 1505.8823; found 1506.8900 $(M+H)^+$. **^{1}H-NMR** (600 MHz, 30% TFA D_2O:H_2O, 1:9) and **^{13}C-NMR** (150 MHz, 30% TFA D_2O:H_2O, 1:9) in Table S5 (Supporting information).

Protease susceptibility assays

Stock solutions of proteinase K were prepared in tris-buffered saline (TBS buffer) (50 μg/mL based on weight to volume). Stock solutions of the linear peptide **2** and amide-bridge cyclic analogue **11** (100 μM) were prepared using 10% DMSO in TBS buffer (pH = 7.6, Aldrich). For the proteolysis reaction, the former peptide stock solutions (200 μL) were mixed with TBS (120 μL). Then, proteinase K stock solution (80 μL) was added (final concentration enzyme 10 μg/mL), the solution mixed, and finally allowed to proceed at room temperature with orbital shaking. Then, the enzymatic reaction was quenched (50 μL) at the desired time point (0, 5, 15, 30, 60, 180 and 300 min for linear peptide **2** and 0, 15, 30, 60, 120, 240, 360, 480 min and 24 h for cyclic analogue **11**) by addition of 1% TFA in water/acetonitrile 1:1 (100 μL). 30 μL of the resulting quenched reaction was injected onto an HPLC-MS (through a HPLC-waters 12695 connected to a Waters Micromass ZQ spectrometer), and the amount of starting peptide present was quantified by mass integration of the peak at 214 nm. Duplicate or triplicate reactions were run for each time point reported

and half-lives were determined by fitting time dependent peptide concentration to an exponential decay using GraphPad Prism.

NMR structural study of peptides 8a and 11

Due to poor water-solubility, samples of peptides **8a** and **11** were prepared at a 1-2 mM concentration in a solution of deuterated TFE/H_2O/D_2O 9:1 30:63:7 in volume at pH 5.5. This pH was selected because amide NH signals are more intense and sharper at pH 5.5 than at pH 7.0, and the pK_a values for the charged side chains in these peptides (Glu & Lys) lie out of this pH range. Hence, peptide conformation will be the same within this pH range. 1D ^{1}H spectra, 2D homonuclear (^{1}H,^{1}H-COSY, 60 ms ^{1}H,^{1}H-TOCSY, and 150 ms ^{1}H,^{1}H-NOESY) spectra, and 2D heteronuclear ^{1}H,^{13}C-HSQC spectra at natural ^{13}C abundance were acquired as previously described[38] using a Bruker AV-600 spectrometer operating at a ^{1}H frequency of 600.13 MHz and equipped with a cryoprobe. Data were processed using the TOPSPIN program.[39] ^{1}H- and ^{13}C-NMR chemical shifts (δ) were assigned following the standard sequential assignment method[40] using the SPARKY software.[36]

Distance constraints for structure calculation were derived from 2D NOESY spectra. The automatic integration subroutine of the Sparky program[36] was used to integrate the NOE cross-peaks. Dihedral angle restraints for ϕ and ψ angles were derived from ^{1}H, ^{13}Cα and ^{13}Cβ chemical shifts using the TALOS program.[41] Since TALOS does not include non-natural residues, Nle and the hydrocarbon staple's residues were considered as Lys for this program. Structure calculations were performed using the program CYANA 2.1.[42] First, the non-natural residue Nle and those required for the covalent closure in peptide **8a** (amino acid *(S)*-**3**) and **11** (Glu and Lys of the amide bridge) were generated in the format required for the CYANA library. Then, the standard iterative protocol for automated NOE assignment was run using as input the list of integrated NOE cross-peaks and the full list of chemical

shifts, and as additional restraints, the TALOS-derived ϕ,ψ dihedral angle ranges, and the upper and lower limit restraints required to link residues at positions 4 and 8. The iterative protocol consists of seven cycles of combined automated NOE assignment and structure calculation of 100 conformers per cycle, and a final step of standard annealing calculation of 100 conformers.[43] The ensemble of the 20 lowest target function conformers resulting from were examined and visualised with MOLMOL[44] and PyMOL.

Molecular dynamics (MD) simulations

All possible stapled peptides **5**-**10** analyzed in Table 1 were built using the Cartesian coordinates of the α-helix formed by residues Pro435-Met447 of monomer B of Li-TryR (PDB entry 2JK6) by introducing the all-carbon staple the *Z* isomer of the olefin in the appropriate positions. In all cases, *N*- and *C*-terminal were defined as acetyl carbamate and carboxamide, respectively. All the systems were simulated in the same conditions as described previously.[15] Peptides **5-10** were introduced in a box of TIP3P waters using the tool *tleap*, integrated in the suite of programs AMBER 12.0.[45] To do this, it was previously necessary to calculate the partial charges and force field parameters for the non proteinogenic residues (*S*)-**3**, (*R*)-**4**, and norleucine (Nle). The cut-off distance for the nonbonded interactions was 12 Å and periodic boundary conditions were used. Electrostatic interactions were treated using the smooth particle mesh Ewald (PME) method with a grid spacing of 1 Å. The SHAKE algorithm was applied to all bonds involving hydrogen atoms and an integration step of 2.0 fs was used throughout. The system was progressively relaxed by energy minimizations, heated to 300K, and further simulated up to a total time of 100 ns without any restraint as described previously.[15] As a hypothesis, in all-hydrocarbon stapled peptides the *Z* isomer of the olefin bridge was used. All peptides were simulated with *N*- and *C*-termini protected as acetyl and carboxamide, respectively. The average degree of

theoretical helicity per residue in **5-10** was assessed with the DSSP[46] algorithm along the course of 100-ns MD simulations at 300 K. The linear prototype **2** was simulated under the same conditions for comparative purposes.

To build the peptide:Li-TryR complexes, the corresponding peptide was overlaid onto the Pro435-Met447 α-helix of monomer B in the crystal structure of the enzyme. Then, a 30-ns of unrestrained MD simulation following the general protocol was performed for each system. The total and per-residue binding energy (kcal mol^{-1}) of the peptides with the protein monomer were calculated using the fast and versatile program MM-ISMSA after tacking into account the last 20 ns snapshots of the respective MD simulation.[47]

Dimer quantitation assay

The stability of the Li-TryR dimeric form in the presence of cyclic peptides **5a, 8a** and **11** and linear precursors **1** and **2** was evaluated using the novel Enzyme-Linked ImmunoSorbent Assay (ELISA) recently developed in our laboratory.[15] Briefly a dual (HIS/FLAG) tagged Li-TryR (400 nM) was incubated in a dimerization buffer (200 μL 300 mM NaCl, 50 mM Tris pH 8.0) for 16 h at 37°C with agitation and in a humid atmosphere in the presence of different peptide concentration (10 to 90 μM). Next the plates were washed ten times with TTBS (Tween 0.1%, 2 mM Tris, 138 mM NaCl 138 pH 7.6) and incubated with diluted monoclonal α-HIS HRP conjugated antibody (200 μL, Abcam, Cambridge, UK) in BSA (5%) in TTBS for 1 h at room temperature. The plates were washed once again as previously described and 1,2-phenylenediamine dihydrochloride (OPD) substrate (100 μL, Dako, Glostrup, Denmark) prepared according to manufacturer's instructions was added. The enzymatic reaction was stopped after 10 minutes with H_2SO_4 (100 μL, 0.5 M) and the absorbances were measured at 490 nm in a VERSAmax microplate reader (Molecular Devices, California, USA). All the assays were conducted in triplicate in at least

three independent experiments. Data were analyzed using a non-linear regression model with the Grafit6 software (Erithacus, Horley, Surrey, UK).

Conflict of interest

The authors declare no financial or commercial conflict of interest

Abbreviations

DSSP	Define secondary structure of proteins algorithm
ELISA	Enzyme-Linked ImmunoSorbent Assay
Li-TryR	*Leishmania infantum* trypanothione reductase
MD	Molecular dynamics
RCM	Ring-closing metathesis
RMSD	Root mean square deviation
SPE	Solid-phase extraction
SPPS	Solid phase peptide synthesis.

Acknowledgements

PASM, MAT and HL thank to the Spanish MEC/MICINN for their FPI fellowships. We also thank the Spanish MINECO (Project SAF2012-39760-C02 and CTQ2011-22514), the Comunidad de Madrid (BIPEDD-2-CM ref S-2010/BMD-2457) and the Junta de Comunidades de Castilla la Mancha (Project POII10-0180-7897) for financial support.

Notes and References

[a] *Laboratorio de modelado molecular, Universidad de Alcalá, Unidad Asociada al CSIC, Madrid, Spain*

[b] *Instituto de Química Médica (IQM-CSIC), Madrid, Spain*

[c] *Departamento de Biología de Sistemas, Universidad de Alcalá, Madrid, Spain*

[d] *Instituto Química-Física Rocasolano (IQFR-CSIC), Madrid, Spain*

*** Corresponding author:** Dr. Sonsoles Velázquez, E-mail: iqmsv29@iqm.csic.es, Phone: (+34) 91 2587458, Fax: (+34) 91 5644853

† Electronic supplementary information (ESI) available

1. WHO. Wold Health Organization, 2013. Available in http://www.who.int/topics/lesihmaniasis/en/ (accessed September 2013).

2. a) N. Singh, M. Kumar and M., R. K. Singh, *Asian Pacific J. Trop. Med.*, 2012, **5**, 485; b) H. Hussain, A. Al-Harrasi, A. Al-Rawahi, I. R. Green and S. Gibbons, *Chem. Rev.,* 2014, **114**, 10369.

3. M. Zucca, S. Scutera and D. Savoia, *Curr. Med. Chem.,* 2013, **20**, 502.

4. K. Ait-Oudhia, E. Gazanion, B. Vergnes, B. Oury and D. Sereno, *Parasitology Research*, 2011, **109**, 1225.

5. T. T. H. Pham, P. M. Loiseau and G. Barratt, *International journal of pharmaceutics,* 2013, **454**, 539.

6. A. H. Fairlamb, P. Blackburn, P. Ulrich, B. T. Chait and A. Cerami, *Science*, 1985, **227**, 1485.

7. R. L. Krauth-Siegel, H. Bauer and R. H. Schirmer, *Angew. Chem. Int. Chem.,* 2005, **44**, 690.

8. See for example, L. S. C. Bernades, C. L. Zani and I. Carvalho, *Curr. Med. Chem.,* 2013, **20**, 2673, and references therein.

9. See for example: a) T. J. Benson, J. H. Mckie, J. Garforth, A. Borges, A. H. Fairlamb and K. T. Douglas, *Biochemical Journal*, 1992, **286**, 9; b) C. Chan, H. Yin, J. Garforth, J. H. McKie, R. Jaouhari, P. Speers, K. T, Douglas, P. J. Rock, V. Yardley, S. L. Croft and A. H. Fairlamb, *J. Med. Chem.,* 1998, **41**, 148; c) M. O. F. Khan, S. E. Austin, C. Chan, H. Yin, D. Marks, S. N. Vaghjiani, H. Kendrick, V. Yardley, S. L. Croft and K. T. Douglas, *J. Med. Chem.,* 2000, **43**, 3148.

10. See also for example: a) J. L. Richardson, I. R. E. Nett, D. C. Jones, M. H. Abdile, I. H. Gilbert, A. H. Fairlamb, S. Patterson, D. C. Jones, E. J. Shanks, J. A. Frearson and P. G. Wyatt, *ChemMedChem,* 2009, **4**, 1333; b) S. K. Venkatesan and D. V. K. Dubey, *Scientific World Journal*, 2012, 1.

11. See for example: a) M. C. O'Sullivan, Q. B. Zhou, Z. Li, T. B. Durham, D. Rattendi, S. Lane and C. J. Bacchi, *Bioorg. Med. Chem.,* 1997, **5**, 2145-2155; b) B. Bonnet, D. Soullez, S. Girault, L. Maes, V. Landry, E. Davioud-Charvet and C. Sergheraert, *Bioorg. Med. Chem.,* 2000, **8**, 95.

12. a) M. R. Ariyanayagam, S. L. Oza, A. Mehlert and A. H. Fairlamb, *J. Biol. Chem.*, 2003, **278**, 27612; b) M. J. Dixon, R. I. Maurer, C. Biggi, J. Oyarzabal, J. W. Essex and M. Bradley, *Bioorg. Med. Chem.,* 2005, **13**, 4513.

13. a) A. Tromelin, M. Moutiez, D. Meziane-Cherif, M. Aumercier, A. Tartar and C. Sergheraert, *Bioorg. Med. Chem. Lett.,* 1993, **3**, 1971; b) E. A. Garrard, E. C. Borman, B. N. Cook, E. J. Pike and D. G. Alberg, *Org. Lett.,* 2000, **2**, 3639.

14. a) S. Patterson, M. S. Alphey, D. C. Jones, E. J. Shanks, I. P. Street, J. A. Frearson, P. G. Wyatt, I. H. Gilbert and A. H. Fairlamb, *J. Med. Chem.,* 2011, **54**, 6514; b) M. H. Duyzend, C. T. Clark, S. L. Simmons, W. B. Johnson, A. M. Larson, A. M. Leconte, A. W. Wills, M. Ginder-Vogel, A. K. Wihelm, J. A. Czechowicz and D. G. Alberg, *J. Enzyme Inhibition and Medicinal Chemistry*, 2012, **27**, 784.

15. M. A. Toro, P. A. Sánchez-Murcia, D. Moreno, M. Ruiz-Santaquiteria, J. F. Alzate, A. Negri, M. J. Camarasa, F. Gago, S. Velázquez, and A. Jiménez-Ruiz, *ChemBioChem*, 2013, **14**, 1212.

16. See for example reviews: a) L. K. Henchey, A. L. Jochim and P. S. Arora, *Curr. Opin. Chem. Biol.,* 2008, **12**, 692; b) A. Grauer and B. König, *Eur. J. Org. Chem.* 2009, 5099; c) R. M. J. Liskamp, D. T. S. Rijkers, J. A. W. Kruijtzer, J. Kemmink, *ChemBioChem,* 2011, **12**, 1626; d) V. Azzarito, K. Long, N. S. Murphy and A. J. Wilson, *Nature Chemistry,* 2013, **5**, 161; e) T. A. Hill, N. E. Shepherd, F. Diness and D. P. Fairlie, *Angew. Chem. Int. Ed.*, 2014, **53**, 13020.

17. See for example review: J. W. Taylor, *Biopolymers*, 2002, **66**, 49.

18. See for example: a) J. C. Phelan, N. J. Skelton, A. C. Braidsted and R. S. McDowell, *J. Am. Chem. Soc.,* 1997, **119**, 455; b) S. G. Yao, M. A. Smith-White, E. K. Potter and R. S. Norton, *J. Med. Chem.,* 2002, **45**, 2310; c) N. E. Shepherd, H. N. Hoang, V. S. Desai, E. Letoize, P. R. Young and D. P. Fairlie, *J. Am. Chem. Soc.*, 2006, **128**, 13284.

19. See for example: a) M. I. García-Aranda, Y. Mirassou, B. Gautier, M. Martín-Martínez, N. Inguimbert, M. Vidal, M. T. García-López, M. A. Jiménez, R. González-Muñiz and M. J. Pérez de Vega, *Bioorg. Med. Chem.*, 2011, **19**, 7526; b) K. K. Khoo, M. J. Wilson, B. J. Smith, M. Zhang, J. Gulyas, D. Yoshikami, J. E. Rivier, G. Bulaj and R. S. Norton. *J. Med. Chem.,* 2011, **54**, 7558; c) M. I García-

Aranda, S. González-López, C. M. Santiveri, N. Gagey-Eilstein, M. Reille-Seroussi, M. Martín-Martínez, N. Inguimbert, M. Vidal, M. T. García-López, M. A. Jiménez, R. González-Muñiz and M. J. Pérez de Vega, *Org. Biomol. Chem.,* 2013, **11**, 1896.

20. See recent reviews: a) A. Brik, *Adv. Synth. Catal.,* 2008, **350**, 1661; b) M. J. Pérez de Vega, M. I. García-Aranda, R. González-Muñiz, *Med. Res. Rev.,* 2011, **31**, 677; c) G. L. Verdine, G. J. Hilinski, K. D. Wittrup and L. V. Gregory, Ed. Elsevier: 2012 Vol 503, pp 3-33; d) R. Dharanipragada, *Future Medicinal Chemistry*, 2013, **5**, 831; e) L. D. Walensky and G. H. Bird, *J. Med. Chem.,* 2014, **57**, 6275.

21. See for example: a) C. E. Schafmeister, J. Po and G. L. Verdine, *J. Am. Chem. Soc.,* 2000, **122**, 5891; b) H. E. Blackwell and R. H. Grubbs, *Angew. Chem. Int.,* 1998, **37**, 3281; c) P. S. Kutchukian, J. S. Yang, G. L. Verdine and E. I. Shakhnovich. *J. Am. Chem. Soc.,* 2009, **131**, 4622.

22. a) F. Bernal, A. F. Tyler, S. J. Korsmeyer, L. D. Walensky and G. L. Verdine, *J. Am. Chem. Soc.,* 2007, **129**, 2456; b) F. Bernal, M. Wade, M. Godes, T. N. Davis, D. G. Whitehead, A. L. Kung, G. M. Wahl and L. D. Walensky, *Cancer cell*, 2010, 411; c) L. D. Walensky, A. L. Kung, I. Escher, T. J. Malia, S. Barbuto, R. Wright, G. Wagner, G. L. Verdine and S. J. Korsmeyer, *Science*, 2004, **305**, 1466; d) L. D. Walensky, K. Pitter, J. Morash, K. J. Oh, S. Barbuto, J. Fisher, E. Smith, G. L. Verdine and S. J. Korsmeyer, Molecular Cell, 2006, **24**, 199; e) N. N. Danial, L. D. Walensky, C-Y. Zhang et al. *Nature Medicine*, 2008, **14**, 144.

23. a) R. E. Moellering, M. Cornejo, T. N. Davis, C. Del Bianco, J. C. Aster, S. C. Blacklow, A. L. Kung, D. G. Gilliland, G. L. Verdine and J. E. Bradner, *Nature*, 2009, **462**, 182; b) G. H. Bird, N. Madani, A. F. Perry, A. M. Princiotto, J. G. Supko, X. He, E. Gavathiotis, J. G. Sodroski and L. D. Walensky, *Proc. Natl. Acad. Sci. USA*, 2010, **107**, 14093; c) T-L. Sun, Y. Sun, C-C. Lee and H. W. Huang, *Biophys.*

J., 2013, **104**, 1923; d) Y-Q. Long, S-X, Huang and Z. Zawahir, *J. Med. Chem.,* 2013, **56**, 5601; e) H-K. Cui, J. Qing, Y. Guo, Y-J. Wang, L.J. Cui, T-H. He, L. Zhang and L. Liu, *Bioorg. Med. Chem.,* 2013, **21**, 3547.

24. The nomenclature $S_{i,i+4}S(8)$ refers to a 8-carbon tether with *S*-configuration at both *i, i+4* positions.

25. The nomenclature $R_{i,i+7}S(11)$ refers to a 11-carbon tether with *R*-configuration at *i, i+4* position and *S*-configuration at *i, i+7* position.

26. Y. W. Kim and G. L. Verdine, *Bioorg. Med. Chem.,* 2009, **19**, 2533.

27. R. M. Williams and M. N. Im, *J. Am. Chem. Soc.,* 1991, **113**, 9276.

28. A. J. Robinson, J. Elaridi, B. J. Van Lierop, S. Mujcinovic and W. R. Jackson, *J. Pep. Sci.,* 2007, **13**, 280.

29. The spectra of peptides **8a** and **11** could not be carried out in absence of TFE due to poor water-solubility of the peptides. It should be noted that TFE is not a general α-helix-inducer, as generally believed (see reference: M. Buck, *Q. Rev. Biophys.*, 1998, **31**, 297). Indeed, it has been shown to stabilise non-helical structures, such as β-hairpins (see reference: C. M. Santiveri, D. Pantoja-Uceda, M. Rico, M. A. Jiménez, *Biopolymers*, 2005, 79150).

30. a) R. Vila, I. Ponte, P. Suau, M. A. Jiménez, M. Rico, Protein Sci., 2000, **9**, 627; b) M. A. Jiménez, A. C. Barrachi-Saccilotto, E. Valdivia, M. Maqueda and M. Rico, *J. Pept. Sci.*, 2005, **11**, 29.

31. P. Güntert, Automated NMR protein structure calculation with CYANA. *Meth. Mol. Biol.*, 2004, **278**, 353.

32. T. Okamoto, K. Zobel, A. Fedorova, C. Quan, H. Yang, W. J. Fairbrother, D. C. S. Huang, B. J. Smith, K. Deshayes and P. E. Czabotar, *ACS Chem. Biol.,* 2013, **8**, 297.

33. D. J. Derksen, J. L. Stymiest and J. C. Vederas, *J. Am. Chem. Soc.,* 2006, **128**, 14252.

34. During the proteolytic stability studies, opening of the lactam-bridge of analogue **11** was not detected by HPLC-MS which points to the stability of the amide bridge in these conditions.

35. See for example: a) N. E. Shepherd, G. Abbenante and D. P. Fairlie, *Angew. Chem. Int. Ed.*, 2004, **43**, 2687; b) E. N. Murgae, G. Gao, A. Bisello and J. Ahn, *J. Med. Chem.,* 2010, **53**, 6421; c) T. Rao, G. Ruiz-Gomez, T. A. Hill, H. N. Hoang, D. P. Fairlie and J. M. Mason, *PLOS ONE*, 2013, **8**, e59415.

36. T. D. Goddard and D. G. Kneller, SPARKY 3, University of California, San Francisco.

37. a) J. L. Stymiest, B. F. Mitchell, S. Wong and J. C. Vederas, *Org. Lett.,* 2003, **5**, 47; b) J. L. Stymiest, B. F. Mitchell, S. Wong, J. C. Vederas, *J. Org. Chem.,* 2005, **70**, 7799.

38. C. M. Santiveri, D. Pantoja-Uceda, M. Rico and M. A. Jiménez, *Biopolymers*, 2005, **79**, 150.

39. NMR data and processing software, Bruker Biospin, Kalsruhe, Germany.

40. Wüthrich, K. 1986, NMR of Proteins and Nucleic acids, John Wiley & Sons, New York, 1986.

41. G. Cornilescu, F. Delaglio and A. Bax, *J. Biomol. NMR*, 1999, **13**, 289.

42. P. Guntert, C. Mumemthaler and K. Wutrich, *J. Mol. Biol.,* 1997, **273**, 283.

43. P. Guntert, *Prog. Nucl. Magn. Res. Spect.,* 2004, **43**, 105.

44. R. Koradi, M. Billeter and K. Wuthrich, *J. Mol. Graphics,* 1996, **14**, 51.

45. D. A. Case, T. A. Darden, T. E. Cheatham, C. L. Simmerling, J. Wang, R. E. Duke, R. Luo, R. C. Walker, W. Zhang, K. M. Merz, B. Roberts, S. Hayik, A. Roitberg, G.

Seabra, J. Swails, A. W. Goetz, I. Kolossvary, K. F. Wong, F. Paesani, J. Vanicek, R. M. Wolf, J. Liu, X. Wu, S. R. Brozell, T. Steinbrecher, H. Gohlke, Q. Cai, X. Ye, J. Wang, M. J. Hsieh, G. Cui, D. R. Roe, D. H. Mathews, M. G. Seetin,R. Salomon-Ferrer, C. Sagui, V. Babin, T. Luchko, S. Gusarov, A. Kovalenko, and P. A. Kollman. Amber 12, 2012.

46. C. Sander and W. Kabsch, *Biopolymers*, 1983, **22**, 2577.

47. J. Klett, A. Núñez-Salgado, H. G. Dos Santos, A. Cortés-Cabrera, A. Perona, R. Gil-Redondo, D. Abia, F. Gago and A. Morreale, *J. Chem. Theory Comput.,* 2012, **8**, 3395.